# THE DIURNAL AND SEASONAL VARIATION OF WATER ICE CLOUDS AS OBSERVED BY EMIRS

**S. A. Atwood**, *Space and Planetary Science Center, and Department of Earth Sciences, Khalifa University, Abu Dhabi, UAE*, *Laboratory for Atmospheric and Space Physics, University of Colorado Boulder, Boulder, USA (Samuel.Atwood@lasp.colorado.edu)*, **M. D. Smith**, *NASA Goddard Space Flight Center, Greenbelt, MD, USA,* **K. Badri,** *Mohammed Bin Rashid Space Center, Dubai, UAE,* **C. S. Edwards**, **N. Smith**, *Northern Arizona University, Flagstaff, AZ, USA,* **P. R. Christensen, S. Anwar**, *Arizona State University, Tempe, AZ, USA,* **M. J. Wolff**, *Space Science Institute, Boulder, CO, USA,* **F. Forget**, *Laboratoire de Météorologie Dynamique, Jussieu, Paris, France,* **M. R. El-Maarry**, *Space and Planetary Science Center, and Department of Earth Sciences, Khalifa University, Abu Dhabi, UAE*

**Introduction:** A considerable record of Martian water ice cloud observations has now been produced from the combined measurements of numerous Mars missions. However, much of this record is derived from sun-synchronous spacecraft that observe at roughly the same local time across their domain (typically early afternoon) or surface instruments with no spatial coverage beyond the lander location. Where local time variable observations of water ice cloud exist, spatial, temporal, or seasonal coverage is often limited. Such bounds to observational coverage hinder efforts to develop Mars atmospheric climatologies, validate global circulation models, and resolve observational anomalies (Clancy *et al.*, 2017).

The Emirates Mars Infrared Spectrometer (EMIRS)—a thermal-infrared spectrometer onboard the Emirates Mars Mission (EMM) spacecraft capable of retrieving water ice cloud column optical depths—observes across all local times and a wide range of latitudes and longitudes, yielding broad coverage at relatively short timescales on the order of two weeks. EMM began science operations in May 2021 near the beginning of Mars aphelion-season, a period of the Martian year during which equatorial water ice clouds are prevalent (Smith, 2004; Clancy *et al.*, 2017).

Here, we present initial results of EMIRS water ice cloud optical depth retrievals focused on diurnal variability during the aphelion season (nominally $L_s$ 40°–140°). Additionally, we compare EMIRS observations against modeled water ice cloud abundances from the *Laboratoire de Météorologie Dynamique* (LMD) global circulation model (GCM), and discuss drivers of diurnal variability in both the equatorial aphelion cloud belt (ACB) and orographic clouds associated with volcanoes.

**EMIRS Data and Methods:** The EMIRS thermal-infrared spectrometer observes Mars with a spectral range of 6.0 to ~100 μm (1666 to ~100 $cm^{-1}$) at typical resolutions of 5 or 10 $cm^{-1}$. The spacecraft is in a low-inclination, 55-hour period elliptical orbit that varies from approximately 20,000 to 43,000 km. Regular raster scans of the Martian disk occur throughout the orbit, with observation footprint sizes ranging from ~100–300 km on the surface (Almatroushi *et al.*, 2021; Edwards *et al.*, 2021).

The EMIRS retrieval follows the algorithm described by Conrath et al. (2000) and Smith et al. (2004), using a constrained linear inversion to sequentially fit the atmospheric temperature profile, dust and water ice column optical depths, and water vapor column abundance. Important to this method is the existence of sufficient thermal contrast between the atmosphere and surface to distinguish between the spectral features of atmospheric constituents. As EMIRS observations span a range of local times this contrast varies, typically reaching the lowest values near dawn and dusk. Consequently, the EMIRS retrieval includes fitting of both the 40 μm (250 $cm^{-1}$) and 12 μm (825 $cm^{-1}$) water ice features. The 40 μm feature occurs in a region of the spectrum with more observed radiance and therefore higher signal-to-noise ratio for fitting purposes as compared to the 12 μm feature, especially at colder temperatures.

EMIRS observational coverage for analyses shown here began with the start of EMM science operations at $L_s$ 48° and included all data through $L_s$ 140°. A gap in observations occurred between approximately Ls 100°–120° due to solar conjunction and a spacecraft safe mode event, during which the peak in ACB optical depths (typically around $L_s$ 105°) likely occurred. Aphelion-season water ice optical depth averages were first filtered to remove spectra with emission angles greater than 70°, or retrieved surface temperatures below 190 K—limiting the results shown here largely to daytime hours. Additional work to retrieve aerosol optical depths at lower surface temperatures is ongoing.

**Results and Discussion:** The spatial distribution of aphelion-season averaged water ice cloud optical depths is shown for local true solar times (LTST) between 0700 and 1700 in Figure 1. The ACB was clearly detectable at all daytime hours, and was generally observed within the band between 10°S and 30°N (black dashed lines) that is often used to bound the ACB latitudinal extents, particularly during afternoon hours. Longitudinal variability was also evident including higher optical depths over Tharsis and lower values just east of the prime meridian. These observations of the ACB were consistent with

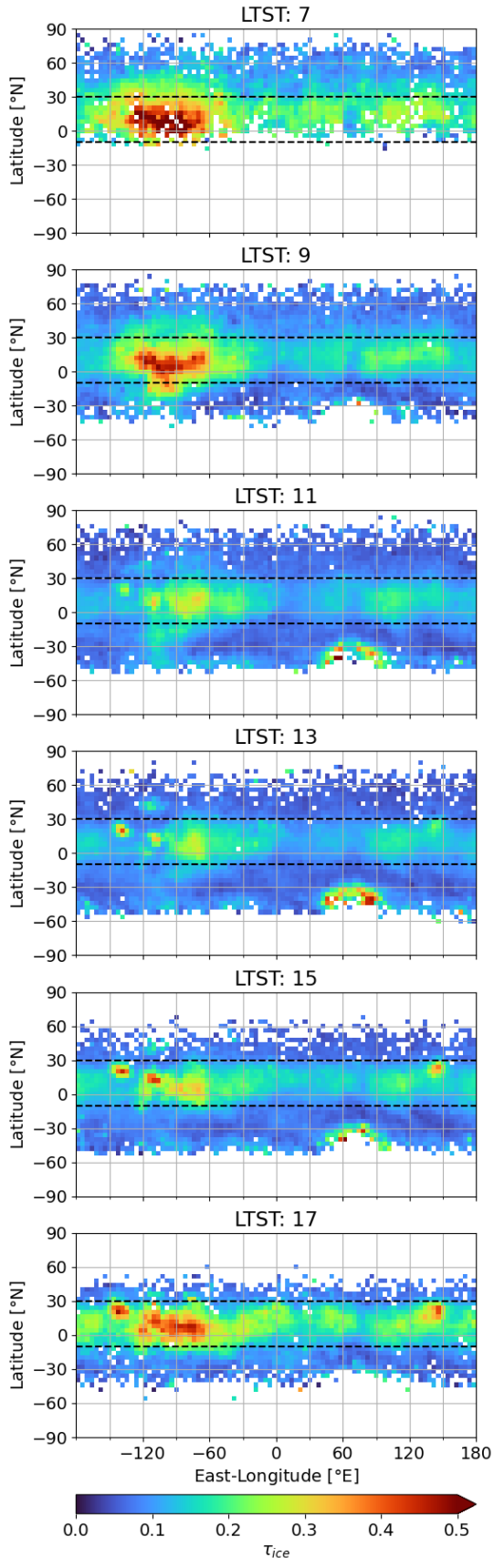


**Figure 1** EMIRS aphelion-season averaged water ice cloud optical depths for six local times. Bins of 2-hr LTST, 4°x4° latitude-longitude averages were smoothed by 2-D Gaussian kernel convolution.

previous observations (Smith, 2004, 2009; Clancy *et al.*, 2017; Wolff *et al.*, 2019; Giuranna *et al.*, 2021), however, variability in local time indicates somewhat more complex behavior as compared to results derived primarily from mid-afternoon observations.

Throughout much of the ACB the average diurnal minimum in optical depth occurred near midday, with higher values often occurring both in the morning and afternoon. Zonal averages produced minima between 1200–1300 LTST—though spatial differences in the timing of the minimum varied between 0900 and 1500, complicating this simple notion of a general midday ACB minimum to some extent. Seasonal changes typically involved scaling in magnitude as higher optical depths were observed closer to the aphelion-season maximum around $L_s$ 105°, but with less of an effect on the relative diurnal pattern. The primary exception to this occurred late in aphelion season when early morning clouds tended to extend further north and south of the nominal ACB latitude band.

Distinctions in the diurnal behavior of water ice clouds were detectable in the vicinity of volcanoes where orographic clouds form due to upslope winds and lee waves propagating off the high elevation peaks (Michaels *et al.*, 2006). In the early morning these clouds were often absent or not detectable above the more spatially extensive ACB cloud signal. As the morning ACB clouds decreased small regions of cloud development were observed by

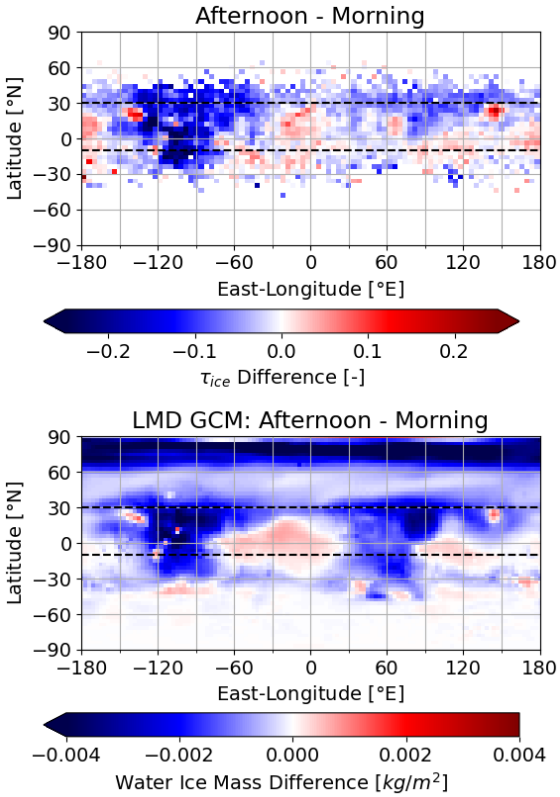


**Figure 2** Diurnal difference between aphelion-season averaged afternoon and morning optical depth for EMIRS observations (top) and LMD GCM output (bottom). Blue (red) indicates morning optical depths were higher (lower) than afternoon values.

midday over Olympus Mons, Tharsis Montes, and Elysium Mons. Orographic cloud optical depths continued to increase throughout the afternoon with no indication of a maxima having been reached by dusk when diurnal coverage ends in this analysis. Some indication of similar behavior was also evident over Alba Patera, though with more limited observational coverage making the signal less evident.

Further investigation of spatial differences in diurnal behavior was conducted through a simple parameterization of the difference in average optical depth between morning and afternoon, shown for regions with sufficient diurnal coverage in Figure 2. Regions with higher optical depths in the morning as compared to the afternoon (blue colors) were particularly evident over the Tharsis region, where early morning clouds extended beyond the nominal bounds of the ACB. A latitudinal extension of water ice cloud beyond afternoon ACB observations has been discussed previously (Heavens *et al.*, 2010; Pankine *et al.*, 2013; Wolff *et al.*, 2019; Guha *et al.*, 2021). This was particularly evident after $L_s$ 120°, implying some seasonal variability in ACB diurnal behavior beyond simple changes to the magnitude of the optical depth. Conversely, the higher afternoon optical depths (red colors) seen for orographic volcano clouds were noteworthy for their high contrast in diurnal signal when compared to the morning dominated ACB clouds in surrounding regions.

A similar parameterization of differences in water ice mass between morning and afternoon was generated for LMD GCM output using roughly the same set of seasonal time periods as the EMIRS observations, allowing for a qualitative comparison to EMIRS results. The spatial distribution for this parameterized diurnal signal was in general agreement between EMIRS and LMD GCM output for both ACB and orographic volcano clouds. Interestingly, the alternating wave-like pattern of morning and afternoon peaks throughout the ACB was also broadly similar. Model simulations have attributed much of the spatial and diurnal patterns in these ACB clouds to thermal tides and associated topographic effects (Hinson and Wilson, 2004; Clancy *et al.*, 2017; Szantai *et al.*, 2021). Qualitative differences were present in some regions, particularly north of Hellas around 20°N latitude where the LMD GCM was higher in the early morning as compared to EMIRS observations. Given that morning observations are generally less available in the observational record of Martian water ice clouds, additional work to investigate the both the retrieval and model behavior in this region and local time may be of interest.

Finally, among previously reported local time variable observations of aphelion water ice cloud, similar trends in optical depths have been noted for increasing afternoon ACB optical depths (Benson *et al.*, 2003; Smith, 2019), midday ACB minima (Akabane *et al.*, 2002; Tamppari *et al.*, 2003; Giuranna *et al.*, 2021), and higher afternoon values for orographic volcano cloud regions. The additional spatial, diurnal, and seasonal coverage provided by EMIRS extends this observational record and adds detail to the current understanding of diurnal trends in Mars aphelion water ice cloud development.

**Acknowledgements:** SAA is supported by the grant (8474000332-KU-CU-LASP Space Sci.)

**References:**

Akabane, T. et al. (2002) 'Diurnal variation of Martian water-ice clouds in Tharsis region of the low latitude cloud belt: Observations in 1995–1999 apparitions', Astronomy & Astrophysics, 384(2), pp. 678–688. doi:10.1051/0004-6361:20020030.

Almatroushi, H. et al. (2021) 'Emirates Mars Mission Characterization of Mars Atmosphere Dynamics and Processes', Space Science Reviews, 217(8), p. 89. doi:10.1007/s11214-021-00851-6.

Benson, J.L. et al. (2003) 'The seasonal behavior of water ice clouds in the Tharsis and Valles Marineris regions of Mars: Mars Orbiter Camera Observations', Icarus, 165(1), pp. 34–52. doi:10.1016/S0019-1035(03)00175-1.

Clancy, R.T. et al. (2017) 'Mars Clouds', in The Atmosphere and Climate of Mars. Cambridge University Press.

Conrath, B.J. et al. (2000) 'Mars Global Surveyor Thermal Emission Spectrometer (TES) observations: Atmospheric temperatures during aerobraking and science phasing', Journal of Geophysical Research: Planets, 105(E4), pp. 9509–9519. doi:10.1029/1999JE001095.

Edwards, C.S. et al. (2021) 'The Emirates Mars Mission (EMM) Emirates Mars InfraRed Spectrometer (EMIRS) Instrument', Space Science Reviews, 217(7), p. 77. doi:10.1007/s11214-021-00848-1.

Giuranna, M. et al. (2021) 'The current weather and climate of Mars: 12 years of atmospheric monitoring by the Planetary Fourier Spectrometer on Mars Express', Icarus, 353, p. 113406. doi:10.1016/j.icarus.2019.113406.

Guha, B.K., Panda, J. and Wu, Z. (2021) 'Observation of aphelion cloud belt over Martian tropics, its evolution, and associated dust distribution from MCS data', Advances in Space Research, 67(4), pp. 1392–1411. doi:10.1016/j.asr.2020.11.010.

Heavens, N.G. et al. (2010) 'Water ice clouds over the Martian tropics during northern summer', Geophysical Research Letters, 37(18). doi:10.1029/2010GL044610.

Hinson, D.P. and Wilson, R.J. (2004) 'Temperature inversions, thermal tides, and water ice clouds in the Martian tropics', Journal of Geophysical Research: Planets, 109(E1). doi:10.1029/2003JE002129.

Michaels, T.I., Colaprete, A. and Rafkin, S.C.R. (2006) 'Significant vertical water transport by mountain-induced circulations on Mars', Geophysical Research Letters, 33(16). doi:10.1029/2006GL026562.

Pankine, A.A. et al. (2013) 'Retrievals of martian atmospheric opacities from MGS TES nighttime data', Icarus, 226(1), pp. 708–722. doi:10.1016/j.icarus.2013.06.024.

Smith, M.D. (2004) ‘Interannual variability in TES atmospheric observations of Mars during 1999–2003’, Icarus, 167(1), pp. 148–165. doi:10.1016/j.icarus.2003.09.010.

Smith, M.D. (2009) ‘THEMIS observations of Mars aerosol optical depth from 2002–2008’, Icarus, 202(2), pp. 444–452. doi:10.1016/j.icarus.2009.03.027.

Smith, M.D. (2019) ‘Local time variation of water ice clouds on Mars as observed by THEMIS’, Icarus, 333, pp. 273–282. doi:10.1016/j.icarus.2019.06.009.

Szantai, A. et al. (2021) ‘Martian cloud climatology and life cycle extracted from Mars Express OMEGA spectral images’, Icarus, 353, p. 114101. doi:10.1016/j.icarus.2020.114101.

Tamppari, L.K., Zurek, R.W. and Paige, D.A. (2003) ‘Viking-era diurnal water-ice clouds’, Journal of Geophysical Research: Planets, 108(E7). doi:10.1029/2002JE001911.

Wolff, M.J. et al. (2019) ‘Mapping water ice clouds on Mars with MRO/MARCI’, Icarus, 332, pp. 24–49. doi:10.1016/j.icarus.2019.05.041.